Journal of Alloys and Compounds 509 (2011) 5250–5255

Contents lists available at ScienceDirect

Journal of Alloys and Compounds

journal homepage: www.elsevier.com/locate/jallcom

Influence of the oxygen content and the preparation method on the power factor of $PrBaCo_2O_{5+\delta}$ samples ($0.54 \leq \delta \leq 0.84$)

B. Rivas-Murias[a,1], M. Sánchez-Andújar[a], J. Rivas[b], M.A. Señarís-Rodríguez[a,*]

[a] Departamento de Química Fundamental, Facultad de Ciencias, Universidad de A Coruña, 15701 A Coruña, Spain
[b] Departamento de Física Aplicada, Facultad de Física, Universidad de Santiago de Compostela, 15782 Santiago de Compostela, Spain

ARTICLE INFO

Article history:
Received 29 July 2010
Received in revised form
30 December 2010
Accepted 9 January 2011
Available online 22 February 2011

Keywords:
Cobalt oxides
Sol–gel synthesis
Electronic transport
Seebeck coefficient
Power factor

ABSTRACT

In this work, we focus on the influence of the oxygen content and the preparation method on the power factor of different $PrBaCo_2O_{5+\delta}$ samples ($0.54 \leq \delta \leq 0.84$). The samples have been initially synthesized by the Pechini method. Their oxygen content has been subsequently modified by annealing under argon/oxygen flow or by electrochemical oxidation/reduction. The oxygen stoichiometry has a high impact on the electrical conductivity and Seebeck coefficient of the resulting materials. Moreover, by adequately reducing their oxygen content while increasing their intergrain conductivity (by increasing the particle size and degree of sintering) the power factor of these samples can be drastically improved. The best result is shown by the $PrBaCo_2O_{5.54}$ sample, that was annealed at high temperature under argon flow, whose power factor is as high as 6.5 $\mu W/K^2\,cm^{-1}$ at ~135 K, more than two orders of magnitude higher than that shown by the initial $PrBaCo_2O_{5.76}$ reference sample.

1. Introduction

The family of compounds $Ln_{1-x}M_xCoO_{3-\delta}$ has been at the center of numerous investigations in the last 60 years since Jonker et al. reported their synthesis in 1953 [1]. In particular, the lanthanum materials have been repeatedly studied in view of their peculiar magnetic and transport properties that change with temperature and upon doping and the spin transitions that take place at the Co ions [2,3]. Their high ionic (O^{2-}) conductivity and possible applications in oxygen permeation membranes, fuel cells, etc. have also attracted a lot of attention [4].

In the mid-nineties, their composition and temperature induced paramagnetic-ferromagnetic and metal-insulator transitions regained increased attention in the search for high magnetoresistance [2,5]. And in this decade some of these materials have been proposed as promising thermoelectric materials due to the discovery of a large Seebeck coefficient [6,7].

As it is well-known, thermoelectric (TE) materials are of interest for power generation from waste heat and for refrigeration [8,9]. Their performance can be evaluated using the figure of merit (Z) defined as:

$$Z = S^2\sigma\kappa^{-1}$$

where S is the Seebeck coefficient of the material, σ its electrical conductivity, and κ its thermal conductivity. The product $S^2\sigma$ is related to electric power for thermoelectric generation and is called the power factor.

A good thermoelectric material should possess a large power factor – that is, a high Seebeck coefficient together with a high electrical conductivity – and a relatively low thermal conductivity, requirements that are not easy to achieve due to the interrelationships among these three parameters.

Nowadays, the best thermoelectric performances are given by intermetallic compounds such as $(Bi,Sb)_2(Te,Se)_3$, filled skutterudites, etc. that present relative high values ($ZT > 1$), but an enhancement of this value is necessary for practical applications [10,11].

Another family of materials that is receiving increased attention is that of ceramic oxides as in addition to the possibility of good thermoelectric behavior, they have the added advantages of higher thermal stability, excellent oxidation resistance, lower cost and weaker toxicity. In this context, Terasaki et al. found [12] that the layered cobalt oxide $NaCo_2O_4$ exhibits a relatively high figure of merit at room temperature, which is comparable to a typical thermoelectric material such as Bi_2Te_3. Since this discovery, many oxidic systems have been investigated, such as $Ca_3Co_4O_9$ [13], $[Bi_{1.68}Ca_2O_4]^{RS}[CoO_2]_{1.69}$ [14,15]. Specially interesting are transi-

* Corresponding author. Tel.: +34 981167000; fax: +34 981167065.
E-mail address: tonasr@udc.es (M.A. Señarís-Rodríguez).
[1] Current address: Departamento de Química-Física y Centro Singular de Investigación en Química Biológica y Materiales Moleculares, Universidad de Santiago de Compostela, 15782 Santiago de Compostela, Spain.

0925-8388/$ – see front matter © 2011 Elsevier B.V. All rights reserved.
doi:10.1016/j.jallcom.2011.01.217

tion metal oxides with highly correlated electrons [16], among them cobalt perovskites $Ln_{1-x}M_xCoO_{3-\delta}$ and related systems, as indicated above.

In this paper, we explore the power factor of cobalt oxides with an oxygen-deficient perovskite-related 112-type structure [17] of formula $PrBaCo_2O_{5+\delta}$. From the structural point of view, these compounds show two main features: the praseodymium and barium ions at the A-site are ordered in alternating (0 0 1) layers resulting in a two-fold superstructure along the *c* axis. In addition, the oxygen vacancies δ, located at the lanthanide (Ln) layers, show a strong tendency to form ordered patterns [17].

As a result, for $\delta = 0$ ($PrBaCo_2O_5$) the structure consists of double-pyramidal cobalt layers containing the barium cations interleaved with lanthanide layers. Meanwhile for $\delta = 0.50$ ($PrBaCo_2O_{5.50}$), the oxygen vacancies order forming filled and empty rows of oxygen sites along *a* axis in the LnO_x planes, resulting in alternating rows of [CoO_5] pyramids and [CoO_6] octahedra that run along the *a* axis, and to an orthorhombic structure with the doubling of the unit cell along the *b* axis [18,19]. Such ordering is also maintained for slightly higher oxygen stoichiometry (up to $\delta = 0.60$), even if for higher oxygen content the system evolves towards a macroscopically tetragonal symmetry due to an inhomogeneous distribution of vacancies in the *ab* plane [19].

As it has been reported, the oxygen content of these materials can change between 5 and 6 ($0 \leq x \leq 1$) depending on the synthesis conditions [17,18,20]. Evenmore, the nature of the oxygen ordering also depends on this parameter [20]. And both factors, the oxygen content and the degree of oxygen ordering, greatly affect the magnetic properties of the resulting materials, as the strength and nature of the magnetic interactions vary depending on the coordination of the Co ions, their mean valence and spin state, as studied in detail by Frontera et al. [18,21,22] and Streule et al. [20] by means of magnetic measurements and neutron diffraction studies [18,20–22].

In this work, we carry out a systematic study to see how the oxygen content and the preparation method influence the transport properties of $PrBaCo_2O_{5+\delta}$ polycrystalline samples and thus their power factor, aspect that to the best of our knowledge has not been previously studied in these compounds.

2. Experimental

The starting compound $PrBaCo_2O_{5.76}$ ($\delta = 0.76$) was prepared by the Pechini method following the procedure described in Ref. [23]. For this purpose, a stoichiometric amount of high-purity Pr_6O_{11} was first converted into the corresponding nitrate by dissolution in HNO_3 (30%). It was then added to a 1 M citric acid aqueous solution, in which stoichiometric amounts of $BaCO_3$ and $Co(NO_3)_2{\cdot}6H_2O$ were also dissolved. The so-obtained solution was diluted and finally ethylene glycol was carefully added in a proportion 10% (v/v). After heating and evaporating the resulting solution at 110 °C, the obtained brown gel was decomposed by heating at 400 °C/1 h. The obtained powder was pressed into pellets and heated in air at 600 °C, 700 °C, 800 °C, 950 °C (with intermediate grindings) and finally at 1000 °C for 45 h followed by a slow cooling to room temperature (0.7 °C/min).

With the aim of obtaining samples with different oxygen contents, this powder was separated into two batches, which were subsequently processed in two different ways:

ANN-series: these samples were given different heating treatments under argon or oxygen flow – see Table 1, followed by a slow cooling to room temperature (1 °C/min).

ELECTR-series: these samples were obtained by electrochemical reduction or oxidation – see conditions in Table 1. Electrochemical experiments were performed using a potentiostat and a three-electrode cell. Our pellets were used as the work-electrode in 1 M KOH aqueous solution. Pt sheet and saturated calomel electrode were the counter and reference electrodes, respectively. The salt bridge was a saturated KNO_3 solution.

All the samples were characterized by powder X-ray diffraction (PXRD) using Cu (Kα) = 1.5418 Å radiation. Rietveld analysis of the powder X-ray diffraction data was carried out using the Rietica software suite [24].

Their morphology and particle size were studied by means of scanning electron microscopy (SEM) using a Jeol 6400 microscope.

Their oxygen content was determined by iodometric titrations. For this purpose, the samples were dissolved in acidified (HCl ~ 5 M) KI solutions, and the I_2 generated was titrated against a thiosulphate solution. All the process was carried out under an argon atmosphere.

Their magnetic properties were studied in a Squid Quantum Design magnetometer. Zero-field-cooled (ZFC) and field-cooled (FC) magnetic susceptibility data were obtained with an applied field of 1 kOe from 5 to 300 K. Hysteresis loops $M(H)$ were obtained at 5 K using fields up to ± 50 kOe.

Their electrical resistivity, ρ, was measured as a function of temperature in the range $78 \leq T(K) \leq 300$ in a zero magnetic field using a dc four-probe method. Seebeck coefficients of pressed pellets were measured in the temperature range $85 \leq T(K) \leq 450$.

Finally, the power factor of these samples (defined as $PF = S^2/\rho$) was calculated from the obtained electrical resistivity and Seebeck coefficient data.

3. Results and discussion

3.1. Sample characterization

According to their room-temperature X-ray diffraction patterns, the obtained $PrBaCo_2O_{5+\delta}$ samples are pure materials in the limit of the detection technique.

Nevertheless, as it will be shown below, two of them ($\delta = 0.64$ and 0.62) contain the desired compound under two different crystal symmetries (tetragonal and orthorhombic).

As for their oxygen content and as expected [18], the samples annealed in oxygen display a higher oxygen content than the reference material (maximum oxygen content is $5 + \delta = 5.84 \pm 0.02$ compared to 5.76 ± 0.02 exhibited by the reference sample, see Table 1). Meanwhile, the treatments under argon flow give rise to samples with lower oxygen contents, with δ values ranging from $\delta = 0.72$ to 0.54 (see Table 1). On the other hand, the ELECTR-samples have $\delta = 0.80$ (after the electrochemical oxidation), $\delta = 0.62$ (after the annealing in argon flow followed by electrochemical oxidation) and $\delta = 0.56$ (after the electrochemical reduction), see Table 1.

As for the morphology of the obtained polycrystalline materials, SEM studies show that the ANN-samples $\delta = 0.84$, 0.80, 0.76, 0.72 and 0.64 and ELECTR-samples $\delta = 0.80$ and 0.56, consist of rather homogeneous and poorly sintered particles with averaged diameter of 1–2 μm (Fig. 1a). Meanwhile, the particle size is larger and the sintering among particles better in the case of the materials annealed in argon during 1100 °C and that show $\delta = 0.54$ and 0.62 (Fig. 1b).

On the other hand, according to PXRD the samples with $\delta \geq 0.72$ (ANN as well ELECTR-samples) display an average tetragonal perovskite structure with cell parameters $\sim a_c \times \sim a_c \times \sim 2a_c$ (space group *P*4/*mmm*). One could be tempted to interpret this result as an inhomogeneous distribution of vacancies in the LnO_x [18]. Nevertheless, this point can only be unambiguously established by neutron diffraction or synchrotron X-ray powder diffraction [18,21] as conventional PXRD data do not really allow to determine if the cell parameters are doubled or not and how is the distribution of the oxygen vacancies.

For example, and on the basis of synchrotron X-ray powder diffraction data obtained from a $\delta = 0.75$ sample (synthesized by solid-state reaction at 1100 °C in air and cooled down to room temperature at 100 °C/h), Frontera et al. [21] concluded that for that composition both the a and b lattice parameters are doubled due to an inhomogeneous distribution of the oxygen vacancies at the 1*b* and 1*d* Wyckoff positions, even if their data sets can be quite well refined using an average structure with cell parameters $\sim a_c \times \sim a_c \times \sim 2a_c$ [21].

Coming back to the here prepared samples, according to PXRD the compounds with lower oxygen content, $\delta = 0.54$ and 0.56 (ANN- and ELECTR-samples, respectively), show orthorhombic symmetry (space group *Pmmm*) and cell parameters $\sim a_c \times \sim 2a_c \times \sim 2a_c$. As indicated in the introduction, the ordering of oxygen vacancies could be giving rise to such orthorhombic symmetry [18,19].

Table 1
Synthesis conditions, oxygen content and cell parameters for the different $PrBaCo_2O_{5+\delta}$ samples.

ANN-samples							
δ	Treatment	T_{treatm} (°C)	Time (h)	Space group	a (Å)	b (Å)	c (Å)
ANN-samples							
0.84	Oxygen annealing	1000	10	*P4/mmm*	3.8977 (1)	3.8977 (1)	7.6392 (2)
0.80	Oxygen annealing	800	12	*P4/mmm*	3.8986 (1)	3.8986 (1)	7.6374 (2)
0.76	Reference sample	1000	45	*P4/mmm*	3.9069 (1)	3.9069 (1)	7.6290 (2)
0.72	Argon annealing	1000	1	*P4/mmm*	3.9083 (1)	3.9083 (1)	7.6260 (2)
0.64	Argon annealing	700	2	*P4/mmm*	3.9132 (2)	3.9132 (2)	7.6220 (3)
				Pmmm	3.9257 (2)	7.8021 (3)	7.6263 (2)
0.54	Argon annealing	1100	2	*Pmmm*	3.9297 (1)	7.8143 (2)	7.6104 (2)

ELECTR-samples							
δ	Treatment	Voltage (V)	Time (h)	Space group	a (Å)	b (Å)	c (Å)
0.80	Electrochemical oxidation	0.4/0.6	20/72	*P4/mmm*	3.9051 (1)	3.9051 (1)	7.6284 (2)
0.62	Ar annealing + Electrochemical oxidation	1100	2	*P4/mmm*	3.9117 (2)	3.9117 (2)	7.6213 (4)
		0.4/0.6	24/48	*Pmmm*	3.9269 (2)	7.8096 (3)	7.6128 (2)
0.56	Electrochemical reduction	−0.3/−0.8	24/24	*Pmmm*	3.9202 (1)	7.8066 (2)	7.6264 (2)

It should be mentioned that the oxygen contents for the appearance of these two symmetries, tetragonal and orthorhombic, in the $PrBaCo_2O_{5+\delta}$ system does fully agree with that reported for the equivalent $GdBaCo_2O_{5+\delta}$ compound [19].

For intermediate oxygen content, $\delta = 0.62$ and 0.64 (ELECTR- and ANN-samples, respectively), the samples consist of a mixture of the just mentioned tetragonal and orthorhombic phases. Such a mixture has also been detected for similar oxygen content in the case of the equivalent $GdBaCo_2O_{5+\delta}$ system, where it has been concluded that it is an intrinsic characteristic of the materials and not a mere consequence of an inhomogeneous or improper annealing [19].

These results vary from those obtained in Ref. [20]. In their work, Streule et al. studied the $PrBaCo_2O_{5+\delta}$ ($0.17 < \delta < 0.79$) system and found an orthorhombic distorsion in all δ range studied by means of conventional PXRD. They conclude that the strength of this orthorhombic distorsion depends on the synthesis history. Around $\delta = 0.5$, the distorsion reaches its maximum value and a doubling of the unit cell along the b direction is necessary. The differences observed with our samples can be caused by their different synthesis history.

On the other hand, the lattice parameters and the variation as a function of oxygen content of our samples are summarized in Table 1. As it can be seen, upon increasing oxygen content the c axis tends to smoothly expand while the a and b parameters tend to slowly contract, as also found in the case of the $GdBaCo_2O_{5+\delta}$ compounds [19].

3.2. Magnetic properties

In order to further characterize the obtained materials, we have measured their magnetic properties and compared them with the behavior previously reported and discussed by other authors on similar samples obtained by different methods [20,22].

In this context and in view of their magnetic behavior (see Fig. 2a and b) we can distinguish three groups of samples in the $PrBaCo_2O_{5+\delta}$ system: samples with (a) $0.76 \leq \delta \leq 0.84$, (b) $0.54 \leq \delta \leq 0.64$ and (c) $\delta = 0.72$ (intermediate behavior).

(a) Samples with $0.76 \leq \delta \leq 0.84$

As expected and in agreement with the data available in the literature [18,21], the starting material, $\delta = 0.76$, shows a magnetic transition at $T_c \sim 135$ K (Fig. 2a and b). The addition of further oxygen results in an increase of the amount of the ferromagnetic component (see Fig. 2a and b) and to a partial suppression of the FM-AFM transition that is known to take place at lower temperature [25].

The FM-PM transition displayed by the $\delta = 0.80$ and 0.84 samples can be explained within a percolating network of FM clusters (oxygen-rich clusters with predominant FM Co^{3+}/Co^{4+} states), when the concentration of oxygen-rich domains exceed a critical value [20].

However, in the case of the $\delta = 0.76$ sample, neutron powder diffraction (NPD) studies should be carried out to confirm this FM behavior. In fact, in the $PrBaCo_2O_{5.75}$ compound Frontera

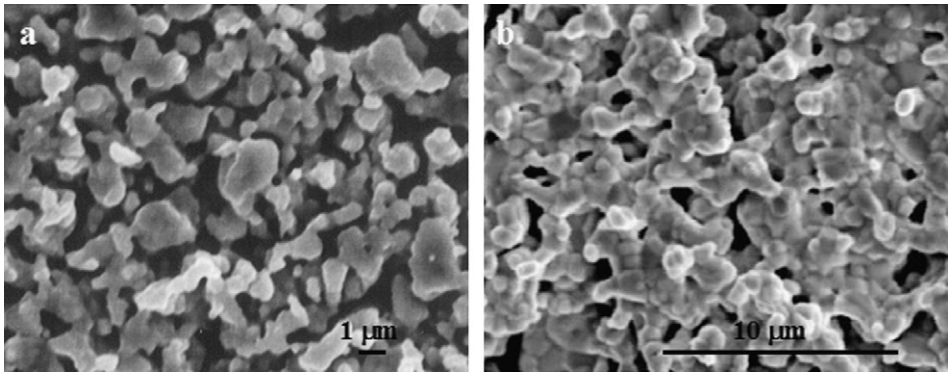

Fig. 1. SEM micrographs for (a) PrBaCo2O5.76 ($\delta = 0.76$ sample) and (b) PrBaCo2O5.54 ($\delta = 0.54$ sample).

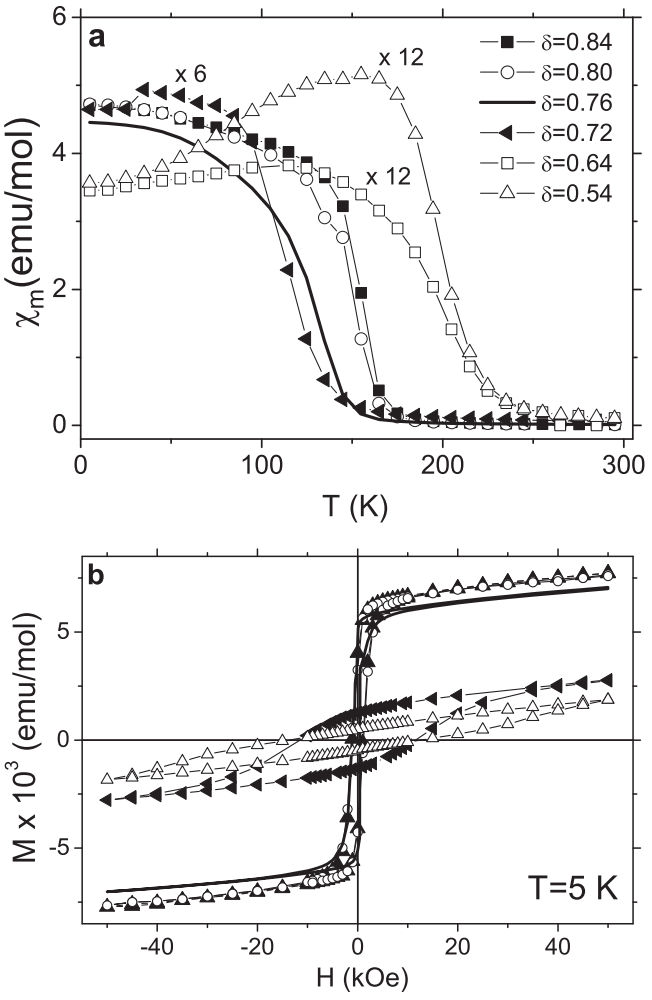

Fig. 2. (a) FC molar magnetic susceptibility under 1 kOe and (b) hysteresis loops at 5 K for $PrBaCo_2O_{5+\delta}$ ANN-samples.

et al. [25,26] found an AF order below ~175 K by means of zero-field NPD measurements, although a FM phase is induced under low field.

(b) Samples with $0.54 \leq \delta \leq 0.64$

The reduction of the oxygen content below $\delta = 0.64$ results in the appearance of a magnetic phase attributed to the compound with $\delta = 0.50$, that presents a net ferromagnetic moment in the cobalt sublattice below 300 K (Fig. 2a), and that at 260 K experiences another FM-AFM transition [21] (see Fig. 2a and b corresponding to the ANN-samples). Further information about the magnetic behavior of $PrBaCo_2O_{5.50}$ compound can be found in Ref. [27].

(c) $\delta = 0.72$ (intermediate behavior)

This sample shows an intermediate behavior between the two groups mentioned above (see Fig. 2a and b).

If we now compare the magnetic behavior of the ANN-samples with that of the ELECTR-samples (not shown), they are essentially similar even if the latter display lower magnetization values. Such difference could be caused by a different degree of oxygen ordering.

3.3. Transport properties

The starting $PrBaCo_2O_{5.76}$ sample shows an almost metallic behavior for $T > 200$ K, with a small resistivity that is almost constant above that temperature ($\rho \sim 1$ mΩ cm) and a small negative thermopower that increases linearly with temperature (Fig. 3). For lower temperatures the resistivity is seen to increase with descending temperatures while the thermopower goes through a maximum centered at 140 K, the critical temperature at which ferromagnetic ordering takes place in the Co–O sublattice (Fig. 2a).

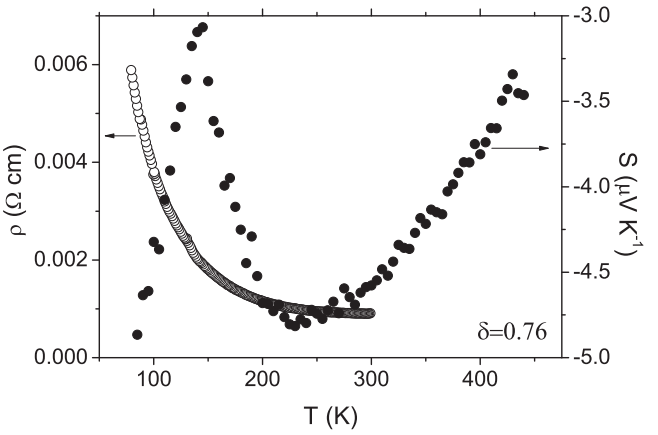

Fig. 3. Temperature dependence of the electrical resistivity (open circles) and thermoelectric power (full circles) for the starting $PrBaCo_2O_{5.76}$ sample ($\delta = 0.76$).

To present and discuss the electrical resistivity and the thermopower of the rest of the samples, we will first refer to their variation as a function of the oxygen content, focusing for this purpose on the ANN-samples series, to then compare the behavior of samples with similar oxygen content but that have been prepared using a different preparation method (ANN-samples vs ELECTR-samples).

As the oxygen content increases above $\delta = 0.76$ and thus the amount of Co^{4+} in the compound, the electrical resistivity of the materials decreases to very small values ($\rho \sim 0.4$ mΩ cm at room temperature) and a metal-insulator transition is detected at the magnetic ordering temperature ($T \sim 150$ K) (see Fig. 4a). As for the thermopower of such samples (Fig. 4b), that of $\delta = 0.80$ and $\delta = 0.84$ is basically similar to that of the starting $\delta = 0.76$ sample, with the difference that the Seebeck coefficient of these two samples goes through a minimum instead of through a maximum at the Curie temperature.

As the oxygen content of the samples decreases below $\delta = 0.76$ and thus their hole doping, the electrical resistivity is seen to rapidly increase below 150 K, specially in the case of $\delta = 0.64$, 0.62 and 0.56 (Fig. 4a). In addition, the resistivity at high temperature tends to an almost constant value for $\delta \geq 0.72$.

This trend is not obeyed by the ANN-sample $\delta = 0.54$ that despite its lowest oxygen shows lower resistivity (Fig. 4a). Nevertheless, it should be remembered that this sample, annealed at higher temperature, shows a higher particle size and a better sintering among particles than the others. This feature results in a better intergrain conduction and in the observed lower resistivity for this sample.

The thermopower of these reduced samples, that is shown in Fig. 4b, is considerable different from that displayed by the more oxygenated ones. As it can be seen, the general trend below 300 K is that the Seebeck coefficient of these samples is positive and markedly increases as temperature and oxygen content decreases. This means that in these samples and in this temperature interval the predominant charge carriers are holes whose number decreases as δ decreases. That is the expected result taking into account that the mean oxidation of the cobalt ions ($2.5 + \delta$) in the samples, or equivalently, the amount of formally Co^{4+} ions, decreases upon diminution of the oxygen content.

The exception to this trend is the samples $\delta = 0.64$ and 0.62 (ANN- and ELECTR-samples, respectively), that even if they display

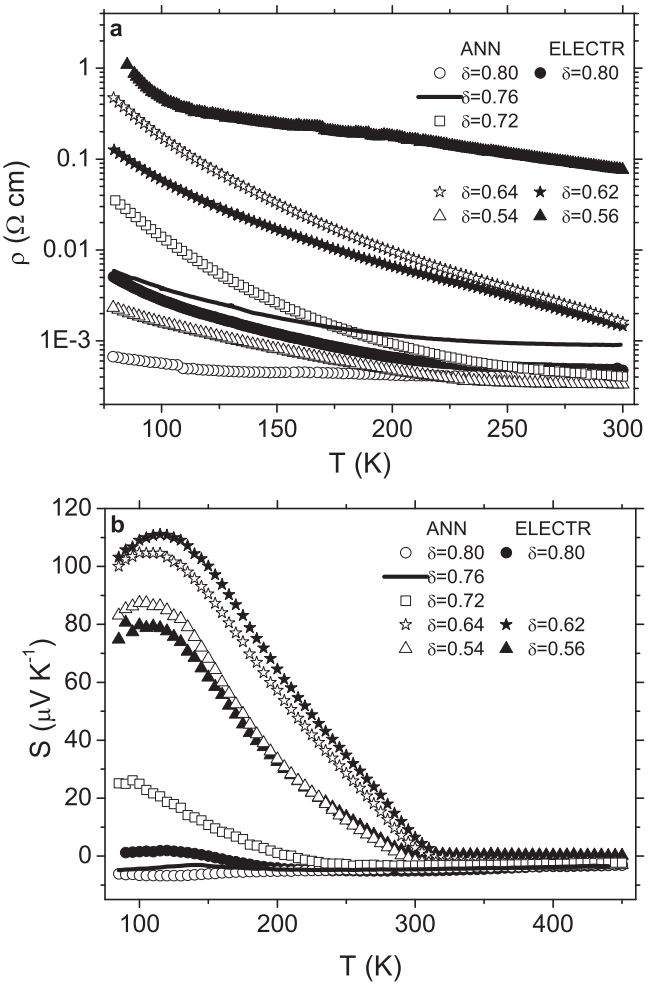

Fig. 4. Temperature dependence of (a) the electrical resistivity and (b) the thermoelectric power of $PrBaCo_2O_{5+\delta}$ samples. ANN and ELECTR are annealing and electrochemical samples, respectively. ×6 and ×12 means that the obtained values were multiplied six- and twelve-times to compare easier.

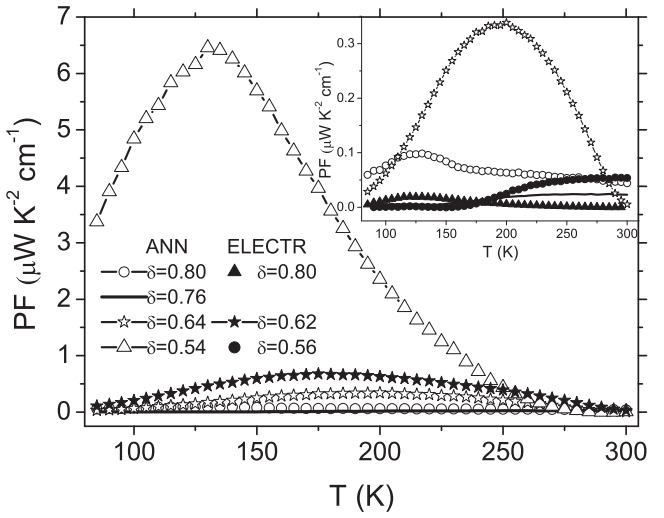

Fig. 5. Temperature dependence of the power factor of all $PrBaCo_2O_{5+\delta}$ samples. Inset: Detail of the power factor of samples $\delta = 0.80$ (ANN- and ELECTR-samples), $\delta = 0.76$, $\delta = 0.64$ and $\delta = 0.56$.

a higher average oxygen content than the samples $\delta = 0.54$ and 0.56 (ANN- and ELECTR-samples, respectively) show a higher Seebeck coefficient. The fact that these $\delta = 0.64$ and 0.62 samples consist of a mixture of an orthorhombic and a tetragonal phase can account for this behavior. The orthorhombic phase probably shows a lower hole doping than that indicated by the average formula and dominates the thermopower behavior at low temperatures, giving rise to higher α values than expected.

For $T > 300$ K the Seebeck coefficient of these reduced samples ($\delta < 0.76$) converges to the same values, that is also very similar to than shown by the more oxygenated ones, and they show a metallic behavior (see Fig. 4b).

To try to understand the transport properties of the reduced samples at low temperatures, we have analyzed the obtained electrical and thermopower data on the basis of different possible models, among them the conventional behavior of band-gap materials, polaronic conduction, Mott's variable range hopping (VRH) or Effros–Shkolovskii type hopping [28,29].

Nevertheless, the transport mechanism is complex and it does not satisfy completely any of the above models, as poor fittings even for small temperature intervals are always found. Such a situation has also been reported to occur in other cobaltite systems [30].

If we now compare the transport properties of samples with similar oxygen content but prepared by different methods (ANN-samples vs ELECTR-samples), we observe the following:

They show similar values of the Seebeck coefficient (see Fig. 4b), which implies that they show similar intragrain conductivity, i.e., the same number of charge carriers. Nevertheless, their electrical resistivity is markedly different (see Fig. 4a). This result can be understood on the basis of a different intergrain conductivity, that can be due to different particle size and/or different degree of sintering as a result of different preparation methods. Thus, a higher particle size and/or a better sintering would enhance the intergrain conduction and give rise to a lower electric resistivity.

In this context, a worsening of the samples sintering upon their immersion in KOH for the electrochemical treatment would explain the substantial increase of the electrical resistivity of, for example, the ELECTR-sample $\delta = 0.80$ as compared to ANN-sample $\delta = 0.80$ (Fig. 4a).

This effect is even more remarkable if compare ANN-sample $\delta = 0.54$ with ELECTR-sample $\delta = 0.56$. In the former the higher sintering temperature used (1100 °C) enhances very significantly the intergranular conductivity, compared to that of the latter, resulting in a material with much lower electric resistivity (Fig. 4a).

If we now compare the behavior of ANN-sample $\delta = 0.64$ with ELECTR-sample $\delta = 0.62$, we see the opposite effect: the electrical resistivity of the latter is smaller than that of the former. Even if this result initially seems to contradict our reasoning so far, in fact it does not, as it should be highlighted that in the case of the ELECTR-sample $\delta = 0.62$, the preparation method involved an annealing at 1100 °C followed by an electrochemical oxidation (see Table 1).

Therefore, the above-mentioned detrimental effect of the electrochemical treatment on the intergrain conductivity is in this case compensated by the better sintering achieved during the treatment at higher temperature, resulting globally in a better conductivity. Nevertheless, and consistently, the achieved improvement in electric conductivity is much less than in the case of the ANN-sample $\delta = 0.54$ where only the favoring effect was present.

From the obtained thermopower and resistivity data we have calculated the power factor of all these samples and compared it with that of the reference $\delta = 0.76$ material. The results are shown in Fig. 5.

As it can be seen, the increase in oxygen content leads to a small improvement of the power factor of the obtained samples as compared to that shown by the reference $\delta = 0.76$ sample due to the diminution of their electric resistivity (i.e., at 200 K PF (ANN-sample

$\delta = 0.80$) ~3.4 times higher and PF (ANN-sample $\delta = 0.84$) ~2.7 times higher).

Nevertheless, a more efficient way to increase the power factor of these samples is to reduce their oxygen content: their power factor increases more than one order of magnitude as the oxygen content gets down to 5.64 (ANN-samples with $\delta = 0.64$ and 0.54).

Evenmore, if simultaneously to the diminution of the oxygen content the particle size of the polycrystalline materials is increased, and their sintering improved, their power factor can be further increase to values as high as 6.5 $\mu W/K^2\,cm^{-1}$ (see Fig. 5), as illustrated by the case of sample ANN-sample $\delta = 0.54$. The drawback is that such high values are only present at low temperatures ($T < 200$ K).

This value of the power factor is comparable to that displayed by $La_{0.90}Sr_{0.10}CoO_3$ [31] even if much smaller than the value reported by Androulakis et al. for $La_{0.95}Sr_{0.05}CoO_3$ [6], who found an unusually large Seebeck coefficient (700 $\mu V\,K^{-1}$ at 300 K).

Although the here shown power factor value is still smaller than those achieved by other thermoelectric materials, the improvement obtained in this work by controlling both the oxygen deficiency and the intergrain conductivity is very interesting and should renew further studies in other systems to optimize their thermoelectric properties.

4. Conclusions

To study the influence of oxygen content and the preparation method on their transport properties and power factor, we have synthesized different $PrBaCo_2O_{5+\delta}$ samples ($0.54 \leq \delta \leq 0.84$) as single-phase materials. The samples have been initially obtained by the Pechini method. Their oxygen content has been subsequently modified by annealing under argon/oxygen flow or by electrochemical oxidation/reduction. According to PXRD the samples with $\delta > 0.72$ present an average tetragonal structure (space group *P*4/*mmm*). Meanwhile, for $\delta = 0.54$ and 0.56 they display an orthorhombic structure (space group *Pmmm*). For intermediate oxygen content ($\delta = 0.62-0.64$) they consist of a mixture of these two symmetries mentioned above. The study of their transport properties (electrical resistivity and Seebeck coefficient) shows the great influence of the oxygen content and preparation method on those properties. Moreover, by adequately reducing their oxygen content while increasing their intergrain conductivity (by increasing the particle size and degree of sintering), the power factor of these samples can be drastically improved. The best result is shown by the $PrBaCo_2O_{5.54}$ sample, that was annealed at high temperature under argon flow, whose power factor is as high as 6.5 $\mu W/K^2\,cm^{-1}$ at ~135 K, more than two orders of magnitude higher than that shown by the initial $PrBaCo_2O_{5.76}$ reference sample.

Acknowledgments

The authors are grateful for financial support from the Spanish Ministry of Education and Science under project MAT2007-66696-C02 and Xunta de Galicia under project 10 PIXB 103 272 PR.

References

[1] G.H. Jonker, J.H. Van Santen, Physica 19 (1953) 120.
[2] G. Briceño, H. Chang, X. Sun, P.G. Schultz, X.-D. Xiang, Science 270 (1995) 273.
[3] H. Masuda, T. Fujita, T. Miyashita, M. Soda, Y. Yasui, Y. Kobayashi, M. Sato, J. Phys. Soc. Jpn. 72 (2003) 873.
[4] Y. Kaga, Y. Ohno, K. Tsukamoto, F. Uchiyama, M.Y. Lian, T. Nakajima, Solid State Ionics 40–41 (1990) 1000, and references therein.
[5] R. Mahendiran, A.K. Raychaudhuri, Phys. Rev. B 54 (1996) 16, 044.
[6] J. Androulakis, P. Migiakis, J. Giapintzakis, Appl. Phys. Lett. 84 (2004) 1099.
[7] T. He, J. Chen, T.G. Calvarese, M.A. Subramanian, Solid State Sci. 8 (2006) 467.
[8] F.J. DiSalvo, Science 285 (1999) 703.
[9] L.E. Bell, Science 321 (2008) 1457.
[10] G. Mahan, B. Sales, J. Sharp, Phys. Today 50 (1997) 42.
[11] D.M. Rowe, CRC Handbook of Thermoelectrics, CRC Press, Boca Raton, FL, 1995.
[12] I. Terasaki, Y. Sasago, K. Uchinokura, Phys. Rev. B 56 (1997) R12685.
[13] M. Mikami, N. Ando, R. Funahashi, Solid State Chem. 178 (2005) 2186.
[14] A. Maignan, S. Hébert, M. Hervieu, C. Michel, D. Pelloquin, D. Khomskii, J. Phys.: Condens. Matter. 15 (2003) 2711.
[15] E. Guilmeau, M. Mikami, R. Funahashi, J. Mater. Res. 20 (2005) 1002.
[16] B.C. Sales, Curr. Opin. Solid State Mater. Sci. 2 (1997) 284.
[17] A. Maignan, C. Martin, D. Pelloquin, N. Nguyen, B. Raveau, J. Solid State Chem. 142 (1999) 247.
[18] C. Frontera, A. Caneiro, A.E. Carrillo, J. Oró-Solé, J.L. García-Muñoz, Chem. Mater. 17 (2005) 5439.
[19] A.A. Taskin, A.N. Lavrov, Y. Ando, Phys. Rev. B 71 (2005) 134414.
[20] S. Streule, A. Podlesnyak, J. Mesot, M. Medarde, K. Conder, E. Pomjakushina, E. Mitberg, V. Kozhevnikov, J. Phys.: Condens. Matter. 17 (2005) 3317.
[21] C. Frontera, J.L. García-Muñoz, A.E. Carrillo, C. Ritter, D. Martín y Marero, A. Caneiro, Phys. Rev. B 70 (2004) 184428.
[22] C. Frontera, J.L. García-Muñoz, O. Castaño, J. Appl. Phys. 103 (2008) 07F713.
[23] B. Rivas-Murias, M. Sánchez-Andújar, A. Fondado, J. Mira, J. Rivas, M.A. Señarís-Rodríguez, NATO Sci. Ser. 61 (2002) 577.
[24] C.J. Howard, B.A. Hunter, Rietica: A computer program for Rietveld analysis of X-ray and neutron powder diffraction patterns, Australian Nuclear Science and Technology Organization Lucas Heights Research Laboratories, 1997.
[25] C. Frontera, J.L. García-Muñoz, A.E. Carrillo, A. Caneiro, C. Ritter, D. Martín y Marero, J. Appl. Phys. 97 (2005) 10C106.
[26] J.L. García-Muñoz, C. Frontera, A. Llobet, A.E. Carrillo, A. Caneiro, M.A.G. Aranda, M. Respaud, C. Ritter, E. Dooryee, J. Magn. Magn. Mater. 272–276 (2004) 1762.
[27] C. Frontera, J.L. García-Muñoz, A.E. Carrillo, M.A.G. Aranda, I. Margiolaki, A. Caneiro, Phys. Rev. B 74 (2006) 054406.
[28] N.F. Mott, Conduction in Non-Crystalline Materials, Oxford University Press, New York, 1993.
[29] B.I. Shklovskii, A.L. Efros, Electronic Properties of Doped Semiconductors, Springer-Verlag, Berlin, 1984.
[30] A.K. Kundu, B. Raveau, V. Caignaert, E.-L. Rautama, V. Pralong, J. Phys.: Condens. Matter. 21 (2009) 056007.
[31] Y. Wang, Y. Sui, P. Ren, L. Wang, X. Wang, W. Su, H.J. Fan, Inorg. Chem. 49 (2010) 3216.